Thermal and Mechanical Properties of Polypropylene–Wood Powder Composites

M. G. Salemane, A. S. Luyt

Department of Chemistry, University of the Free State—Qwaqwa Campus, Phuthaditjhaba 9866, South Africa

Received 20 June 2005; accepted 15 August 2005
DOI 10.1002/app.23521
Published online in Wiley InterScience (www.interscience.wiley.com).

ABSTRACT: The preparation and characterization of modified and unmodified polypropylene (PP)–wood powder (WP) composites were done under fixed processing conditions. Different techniques were used to study the effect of both WP size and content, as well as compatibilizer content, on the properties of the composites. The results point to the fact that, WP settles in the amorphous part of the matrix and creates new crystalline phases or zones. Scanning electron microscopy micrographs show a relatively even distribution of WP in the PP matrix, which contributes to improvements observed in the properties of the material. Hg-porosimetry results indicate that the PP matrix, which has a low pore volume, filled the pores in the WP particles. This reduced the total volume of pores in the PP–WP composites. This observation was also supported by a general decrease in gas permeability of the material. Thermal analysis results indicate that the presence of both WP and maleic anhydride grafted polypropylene (MAPP) leads to an increase in enthalpy (crystallinity) values, but to a decrease in lamellar thickness in the composites. The thermal stability of the composites improves somewhat compared to that of PP. There were distinctive differences between the results for composites containing different WP particle sizes, as well as for composites prepared in the presence and absence of MAPP. It is clear from the results that the presence of MAPP generally improves the tensile properties of the composites. Larger WP particles gave rise to better tensile properties, in the presence and absence of MAPP. J Appl Polym Sci 100: 4173–4180, 2006

Key words: polypropylene; wood powder; differential scanning calorimetry; thermogravimetric analysis; tensile properties; gas permeability; porosity

INTRODUCTION

Natural fillers have recently attracted the attention of scientists and technologists because of the advantages they provide over conventional reinforcement materials, such as glass fibers, talc, mica, etc.[1–3] Natural fillers may be used in the form of particles or bundles, and may act as reinforcement for plastics.[4] Wood flour and other low cost agricultural-based flour can be considered as particulate fillers that enhance the tensile and flexural moduli of the composite, with little effect on the composite strength.[5] Unlike synthetic fibers, e.g., glass fibers, natural fillers can be incinerated after the composite component has served its useful life. The incineration of natural fillers theoretically results in no net addition to CO_2 emissions, because plants, from which these fibers are obtained, sequester atmospheric CO_2 during their growth, which is released during the combustion of natural fillers.[6]

Wood is one of the oldest and most widely used structural material. It is composed of strong and flexible cellulose fibers (linear polymer) surrounded and held together by a matrix of lignin and other polymers.[7] Wood fillers are biodegradable and nonabrasive even after processing, unlike other reinforcing fillers or fibers. Wood flour is one of the most common natural fillers used in the thermoplastics industry. It is produced commercially from postindustrial sources such as plane shavings and sawdust. One of the variable used to characterize wood flour is particle size. This can be obtained by the use of an analytical sieve or a screen that is used to differentiate between particle sizes. However, extra screening of wood flour, for example screening out fines to narrow the particle size distribution, raises the cost of the flour. For this reason, typical commercial grades include a mixture of particle sizes. It was somewhat difficult to characterize the properties of commercial wood flour–plastic composites on the basis of specific particle sizes. When wood flour is used as filler for plastics, it tends to increase the stiffness of the composite, but does not improve its strength.[4]

Aggregation of particles, especially finer particles, is another factor that can influence the final properties of the composite.[8] In most instances aggregation occurs at higher filler contents (20 and 30 wt %) and it overshadows the differences between individual fillers. Very fine filler particles are difficult to disperse, and

Correspondence to: A. S. Luyt (luytas@qwa.uovs.ac.za).

TABLE I
Materials Used and Suppliers

Material	Supplier
Pine wood powder (WP)	FBW Taurus, Phuthaditjhaba, South Africa
Polypropylene (PP)	Sasol Polymers, Johannesburg, South Africa
Maleic anhydride grafted polypropylene (MAPP)	Pluss Polymers Pvt. Ltd., India

the agglomerates then behave as large single particles. Low interfacial adhesion and particle agglomeration initiate crack formation. Fine or small filler particles are found to improve the mechanical properties of polymer composites more than large ones. The only drawback to the use of finer particles is their tendency to agglomerate.[8–10]

Compatibilization is a method that is very often used to control the phase morphology, phase stabilization, and interfacial adhesion in polymer composites and immiscible polymer blends.[11] Most wood powder–plastic composites result in materials with a weak interfacial region, which is found to reduce the efficiency of stress transfer from the matrix to the reinforcement component. In some instances, the addition of wood filler to a polymer gives rise to a concentration of holes, which were left after the fillers were de-bonded from the matrix. This hole proximity indicates that the sawdust fillers exist in the form of bubbles, which could not provide efficient stress transfer from the matrix.[12–14] In natural filler composites, weak adhesion may result from poor dispersion and incompatibility between the hydrophilic natural fillers and the hydrophobic polymer.[14] The use of a compatibilizer can improve adhesion and thus enhance the tensile properties of the composite. Polypropylene/sawdust composites show a change in the properties with increasing maleated polypropylene (MAPP) concentration. These changes are observed at high MAPP content. The composites with MAPP content lower than 20 wt % have lower tensile properties. The improved filler–matrix adhesion observed on the addition of MAPP can be attributed to the esterification reaction between the hydroxyl groups of the cellulose filler and the anhydride functionalities of MAPP.[13,15,16] Interactions between the anhydride groups of the maleated coupling agents and the hydroxyl groups of the natural fillers can overcome the incompatibility problem; thus increasing the tensile and flexural strengths of natural filler–thermoplastic composites.[4] Only a maleated coupling agent with the correct balance of maleic anhydride and molecular weight can achieve peak performance in natural filler composites.[14]

Maleated polyolefins (MaPO) are coupling agents that are used to strengthen composites containing filler and fiber reinforcements.[17] The coupler may co-crystallize with the continuous polyolefin, while the maleic anhydride portion of the molecule can interact with the more polar wood surface. It was suggested that the interaction between the coupler and wood may be of a covalent nature. Mechanical interlocking may occur between the wood and coupler, and the polymer and coupler. All these bonding forms may concurrently exist across the interface at varying degrees. There are other factors influencing the performance of the compatibilizer, i.e., molecular weight and acid number. Low molecular weight will not allow the coupler to interact and entangle sufficiently with the polyolefin phase. Also high molecular weight may not allow the coupler to reside at the interface. A low acid number may not give the coupler enough sites for attachment to the polar filler. Too high an acid number may hold the coupler close to the polar surface and not allow sufficient interaction with the continuous nonpolar phase. Maleated couplers need enough acid functionality to attract the filler and enough molecular weight to entangle or crystallize into the base polymer.

The aim of this study was to determine and explain the influence of wood powder size and content, as well as, the presence and the amount of maleic anhydride grafted polypropylene (MAPP) on the thermal and mechanical properties of polypropylene–wood powder composites.

EXPERIMENTAL

Materials in this work were used as received from the suppliers (Tables I and II). The wood powder was separated into different particle sizes using laboratory test sieves with pore sizes of 600, 300, 150, and 38 μm. Polypropylene (PP) and polypropylene/maleic anhydride grafted polypropylene (PP/MAPP) composites, containing respectively, 10, 20, and 30 wt % wood powder (WP), were prepared with each of these separated wood samples. Samples were weighed according to the desired ratios to make up a total mass of 40 g

TABLE II
Properties of Materials

Properties	WP	PP	MAPP
Density (g cm^{-3})	1.5	0.9	0.91
Melt flow index (MFI) at 230 °C and 2.16 kg (g/10 min)	—	12	55
Melting temperature (T_m) (°C)	—	160	163
Tensile strength at yield (MPa)	—	30	—
Elongation at yield (%)	—	7.5	—
Flexural modulus (MPa)	—	1360	—
Minimum maleic anhydride (MAH) content (%)	—	—	1.0

(which is the mass that is required to thoroughly mix the different components), and mixed in a Brabender Plastograph at 180°C at a speed of 60 rpm for 10 min. Before the mixing, wood powder and MAPP were dried in an oven at 100°C for 24 h and 1 h respectively. Composites with and without MAPP were prepared for further analysis. After preparation, the samples were melt pressed at 190°C for 3 min, and were allowed to cool for 5 min at room temperature.

DSC analyses were carried out on a Perkin–Elmer DSC7 differential scanning calorimeter under flowing nitrogen atmosphere. The calibration of the instrument was done using the onset temperatures of melting of indium and zinc standards, as well as the melting enthalpy of indium. The samples were cut using a standard hollow steel punch to produce uniform samples. Samples (5–10 mg) were heated from 50 to 250°C at a rate of 10°C min^{-1}, held at 50°C for 1 min to eliminate any thermal history effects, cooled to 50°C at the same rate, and reheated. The enthalpies and melting temperatures were determined from the second scan.

TGA analyses were carried out on a Perkin–Elmer TGA7 thermogravimetric analyser. Samples ranging between 10 and 15 mg were heated from 50 to 600°C at a heating rate of 20°C min^{-1} under flowing nitrogen.

Tensile properties were determined using a Hounsfield H5KS tensile tester. At least seven test pieces, with a gauge length of 24 mm, of each sample were analyzed at a speed of 10 mm min^{-1}.

Permeability measurements were done using a Sierra Smart-Trak mass flow meter. To determine the gas permeability of the composites, oxygen at different flow rates was used.

A mercury porosimetry method was used for the evaluation of pore size distributions. The measurements were carried out in a Porozimetro 1500 Carlo Erba instrument connected to a calculation unit CVT 960. The maximum mercury pressure was 150 MPa, which allowed determination of pore sizes down to 5 nm.

The scanning electron microscopy (SEM) analyses were done on a Jeol 6400 WINSEM scanning electron microscopy model at 5 keV.

RESULTS AND DISCUSSION

Figure 1 shows the SEM micrographs of the PP–WP composites. The difference in wood powder particle size is clear from this figure. For composites with small WP particles (<38 μm), the surface is smoother than for the samples containing larger particles (300–600 μm). When MAPP is introduced into the composite material, the surfaces are even smoother. In these photos, there is no clear distinction between WP filler and PP matrix. It, therefore, seems as if the composite mixtures are homogeneous, and that the WP particles

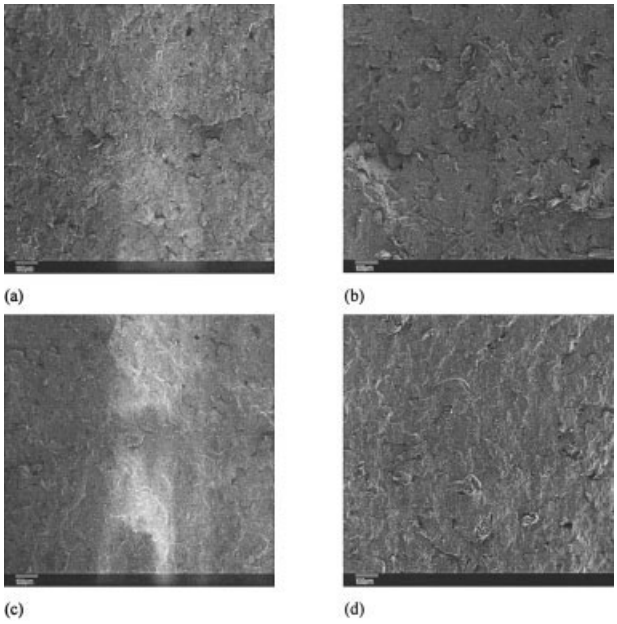

Figure 1 SEM micrographs for modified and unmodified PP/WP composites at ×100 magnification. (a) 60/40 w/w PP/WP (<38 μm), (b) 60/40 w/w PP/WP (300–600 μm), (c) 60/10/30 w/w PP/MAPP/WP (<38 μm), (d) 60/10/30 w/w PP/MAPP/WP (300–600 μm).

are relatively evenly distributed in the polymer matrix.

The Hg–porosimetry results for pure WP, as well as the PP–WP and PP/MAPP–WP composites are shown in Figure 2. WP has a large pore volume. Pores with radii from 10 to 2511 nm take up a relatively large volume, confirming that WP is a very porous material. PP has a relatively large volume of very small pores, but the volume decreases rapidly with increasing pore size. When WP is added into the polymer matrix, the pore size distribution does not change much from that of pure PP. This behavior is in line with the SEM results that indicate that WP is relatively well dispersed into the polymer matrix. The PP seems to completely fill the pores in WP during mixing. The same is observed for composites with 10% MAPP. The smooth surfaces, observed on the SEM micrographs for composites with 10% MAPP, are probably the result of stronger interaction between the matrix and WP. These results point to good interfacial adhesion as a result of mechanical interlocking. This is further emphasized by looking at the mean pore radius at V_p = 50% nm^{-1}. For pure WP the value is 3041.5 nm and for pure PP it is 48.9 nm. These values decrease to 15.0 nm for the PP–WP composite, and to 13.6 nm for the PP/MAPP–WP composite.

It is commonly known that PP has relatively high oxygen permeability.[18] Composites containing WP with particle size <38 μm have a lower gas permeability than pure PP (Fig. 3). Addition of MAPP some-

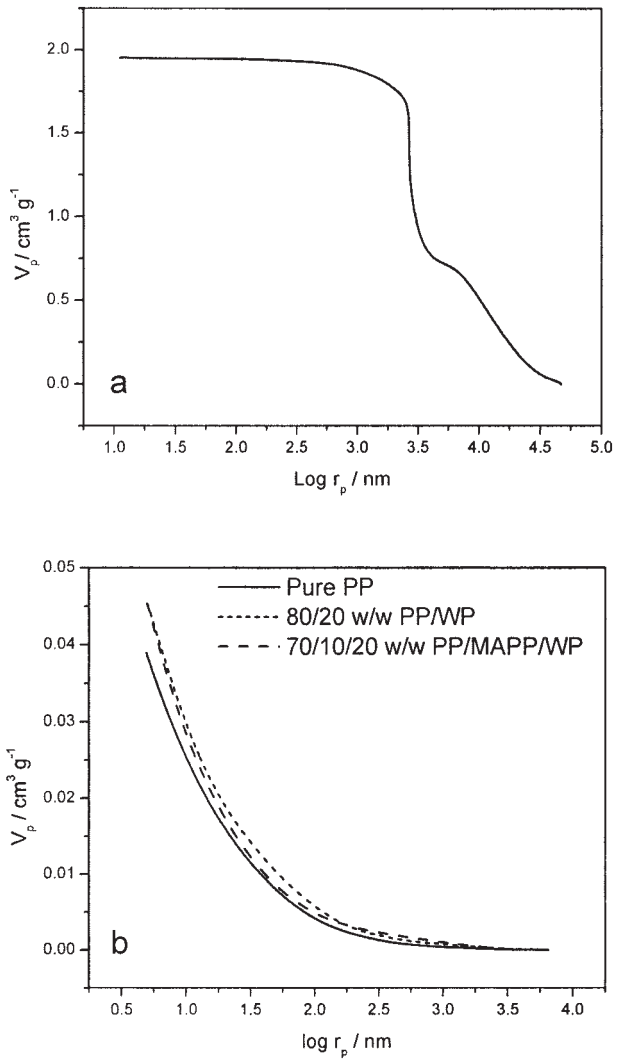

Figure 2 Pore volume as function of pore size for (a) pure WP, and (b) PP and composites containing <38 μm WP.

what increases the permeability, although the effect is very small. This is not only the result of PP and/or MAPP filling the pores in WP, but also of increased crystallinity of the matrix in the presence of WP (see discussion below). It is well known that higher crystallinity gives rise to lower permeability. For composites with large WP particles (300–600 μm), the permeability of oxygen gas is much higher than in the case of composites containing small WP particles, and even higher than that of the pure polymer. In this case, the addition of MAPP led to a slight decrease in the permeability. The increase in crystallinity is similar to that for composites containing the small WP particles, and, therefore, the higher permeability is probably the result of polymer molecules not completely filling the pores in the WP particles. There may also be some cracks at the interface between the WP and the matrix, allowing gas molecules to pass through.

For both the composites containing <38 μm and 300–600 μm WP particles, an increase in WP content

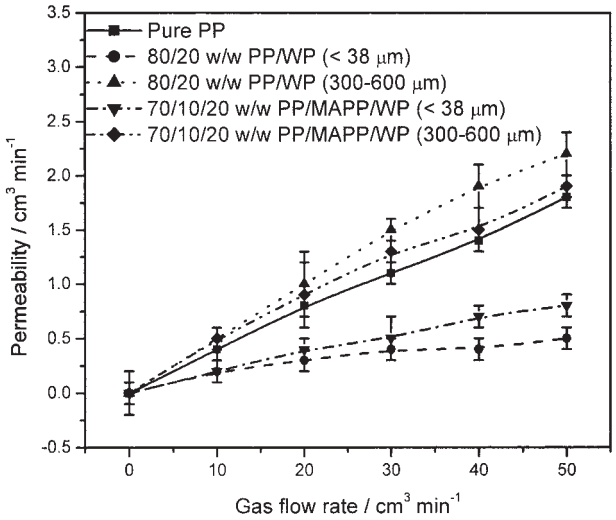

Figure 3 Permeability as a function of oxygen gas-flow rate for composites with and without compatibiliser.

leads to higher enthalpy values compared to the theoretically expected values (Table III), and since enthalpy is proportional to crystallinity, this also indicates an increase in crystallinity of the material. The crystallinities were calculated using eq. (1), with ΔH^*_m = 209 J g^{-1} the specific melting enthalpy for 100% crystalline polypropylene[19]

TABLE III
Summarized DSC Results

PP/MAPP/WP (w/w)	ΔH_m^{obs} (J g^{-1})	ΔH_m^{exp} (J g^{-1})	$T_{o,m}$ (°C)	$T_{p,m}$ (°C)
100/0/0	67.5	—	156.8	164.9
0/100/0	72.1	—	153.2	159.0
90/10/0	72.8	—	151.3	157.5
		—		162.9*
90/0/10 (<38 μm)	60.6	60.8	156.1	162.0
80/0/20 (<38 μm)	63.2	54.0	156.4	163.2
60/0/40 (<38 μm)	63.5	40.5	158.5	163.4
90/0/10 (300–600 μm)	67.4	60.8	157.4	162.4
80/0/20 (300–600 μm)	52.9	54.0	157.8	163.4
60/0/40 (300–600 μm)	53.5	40.5	158.7	163.2
90/0/10 (38–150 μm)	62.9	60.8	156.2	161.7
90/0/10 (150–300 μm)	61.0	60.8	155.8	162.4
85/5/10 (<38 μm)	66.9	60.8	158.7	164.2
80/10/10 (<38 μm)	60.1	45.8	158.1	164.9
70/10/20 (<38 μm)	68.1	42.9	158.6	163.0
60/10/30 (<38 μm)	53.6	43.4	158.2	162.7
85/5/10 (300–600 μm)	63.2	60.8	158.8	163.2
80/10/10 (300–600 μm)	68.3	45.8	158.6	163.4
70/10/20 (300–600 μm)	63.2	42.9	158.8	163.7
60/10/30 (300–600 μm)	64.4	43.4	158.8	163.7
80/10/10 (38–150 μm)	66.0	45.8	156.7	162.0
80/10/10 (150–300 μm)	61.3	45.8	156.1	163.7

ΔH_m^{obs} - experimentally observed melting enthalpy; ΔH_m^{exp} - theoretically expected melting enthalpy; $T_{o,m}$ - onset temperature of melting; $T_{p,m}$ peak temperature of melting: * - peak shoulder.

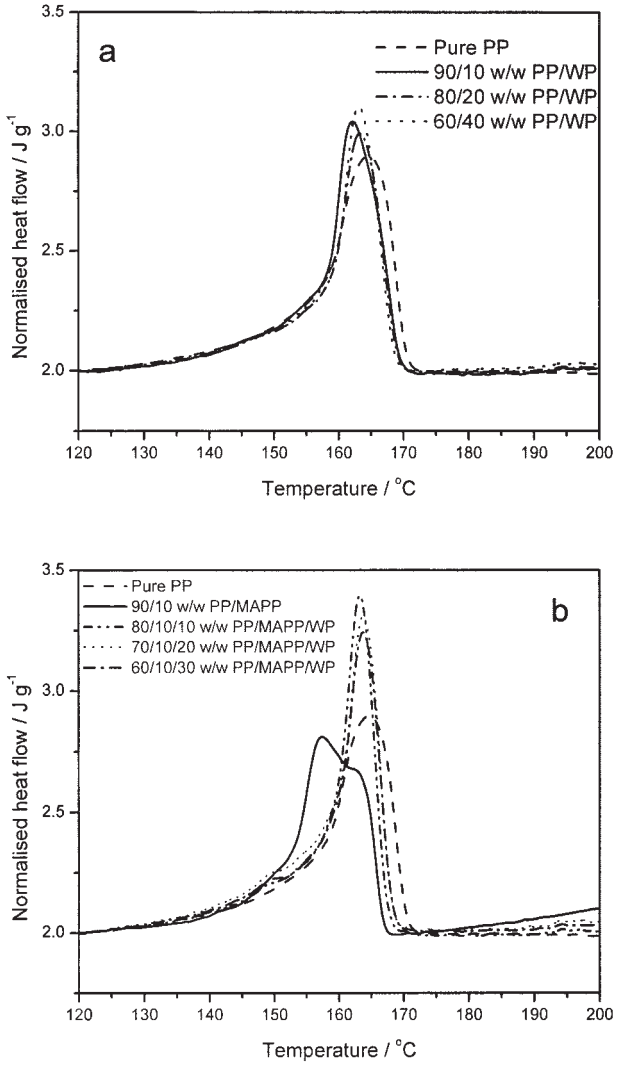

Figure 4 DSC heating curves for composites containing (a) <38 μm WP particles, and (b) <38 μm WP particles and 10% MAPP.

$$X_c = \Delta H / \Delta H_m^{\bullet} \quad (1)$$

where ΔH_m is the specific melting enthalpy of polypropylene. The value increases from 32.3% for pure PP to 35.9 and 40.4% for 90/10 and 80/20 w/w PP/WP, respectively. A possible explanation for this observation is that, when WP is introduced into the PP matrix, it settles in the amorphous region, and as a result new crystalline zones are formed around the WP particles through epitaxial crystallization on their surfaces. For all WP sizes, the peak temperature of melting of the composites are somewhat lower than that of pure PP (Fig. 4 and Table III), indicating a decrease in lamellar thickness, which may also be the result of epitaxial crystallization on the WP surfaces.

The presence of MAPP in the composites does not seem to have a major influence on the enthalpy values or peak temperatures of the composites (Table III). These values are similar to those for composites prepared in the absence of MAPP. It is, however, interesting that the 90/10 w/w PP/MAPP blend shows a double melting peak with peak temperatures at about 157 and 162°C (Fig. 4), while the PP/MAPP–WP composites containing 10 wt % MAPP show only one well defined melting peak at about 164°C. It seems as if in the absence of WP, the MAPP and PP crystallizes into two distinguishable fractions, both at temperatures lower than that of pure PP, indicating the formation of thinner lamellae than those of pure PP. The presence of WP seems to initiate co-crystallization of PP and MAPP into thicker lamellae that melt in the same temperature range than pure PP. This may be the result of a possible interaction between the hydroxyl groups in WP and the anhydride groups in MAPP.

Figure 5 shows the TGA curves of pure PP, pure MAPP, and PP–WP composites with and without MAPP. MAPP is clearly less thermally stable than PP, with almost a 200°C difference between their respective onset temperatures of decomposition (Table IV). The WP powder curve shows more than one decomposition step. At about 60°C, there is dehydration of moisture that was trapped inside the WP particles, and at 314°C the depolymerization of lignocellulosic fibers in WP occurs, followed by further breakage of the chains. Increased WP (<38 μm particle size) content seems to increase the thermal stability of the composites, and only one decomposition step can be observed for low WP contents. This observation is probably the result of higher PP crystallinity in the presence of WP. As the WP content increases to 40%, two decomposition steps are observed. This may result from the high content of WP, which leaves WP particles that are not in intimate contact with PP, and

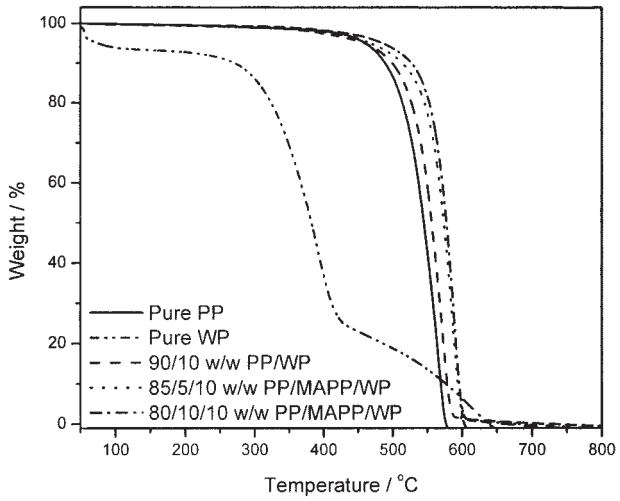

Figure 5 TGA curves for composites containing <38 μm WP particles and different MAPP contents.

TABLE IV
TGA Onset Temperatures of Decomposition

PP/MAPP/WP (w/w)	Onset temp. / °C
100/0/0	498
0/100/0	395
0/0/100	314 / 425 / 648[a]
95/5/0	378
90/10/0	379
90/0/10 (<38 μm)	521
80/0/20 (<38 μm)	529
60/0/40 (<38 μm)	379/525[a]
90/0/10 (300–600 μm)	400/548[a]
80/0/20 (300–600 μm)	402/526[a]
60/0/40 (300–600 μm)	399/524[a]
90/0/10 (38–150 μm)	400/558[a]
90/0/10 (150–300 μm)	403/561[a]
85/5/10 (<38 μm)	537
80/10/10 (<38 μm)	540
70/10/20 (<38 μm)	521
60/10/30 (<38 μm)	502
85/5/10 (300–600 μm)	401/553[a]
80/10/10 (300–600 μm)	480
70/10/20 (300–600 μm)	469
60/10/30 (300–600 μm)	482
80/10/10 (38–150 μm)	539
80/10/10 (150–300 μm)	550

[a] TGA curves show more than one decomposition step.

which will start decomposing before the rest of the composite. Larger WP particles (300–600 μm) in the composites give rise to similar behavior, but here decomposition is a two-step process, even at low WP contents.

In the presence of MAPP, the composite containing 10% of <38 μm WP particles seems to be more thermally stable than either PP or the composites containing higher WP contents (Table IV). The latter composites have almost the same thermal stability as PP. Composites containing larger WP particles (300–600 μm) in the presence of MAPP show a lower thermal stability than that of pure PP. It is, however, still much higher than that of WP alone or the PP/MAPP blends. An increase in MAPP content increases the thermal stability of the composites above that of pure PP, which is the result of stronger interfacial interaction in the presence of MAPP. A similar trend was observed for composites containing 300–600 μm WP particles.

Figure 6 and Table V show a decrease in elongation at break for composites containing 38–150 μm and 300–600 μm WP particle sizes. This indicates that the presence of WP in the matrix reduces the ability of the sample to deform by restricting the mobility of the polymer chains. As a consequence, it is difficult for the segments of the material to easily slip past each other. For the composite containing <38 μm WP, there is a slight increase in elongation at break for the sample containing 10% WP. However, this property slightly decreases in value for higher WP contents. A probable reason is that the particles are almost evenly distributed in the matrix. Since the WP particles are small and of low content, it has little influence on PP chain mobility. As discussed above, the crystallinity of the matrix increases on introduction of <38 μm WP, which restricts the flexibility of the chain segments, leading to a decrease in elongation at break. Elongation at break for composites with 10% MAPP decreases with an increase in WP content. There probably is strong interaction between MAPP and WP particles, even for small particle sizes. This will reduce chain mobility, and decrease elongation at break with increasing WP content.

In Figure 7, a general decrease in the stress at break is observed for all composites. This behavior is not in line with the increase in crystallinity of the material, but probably results from the fact that, due to poor interaction between the polymer and filler, interfacial

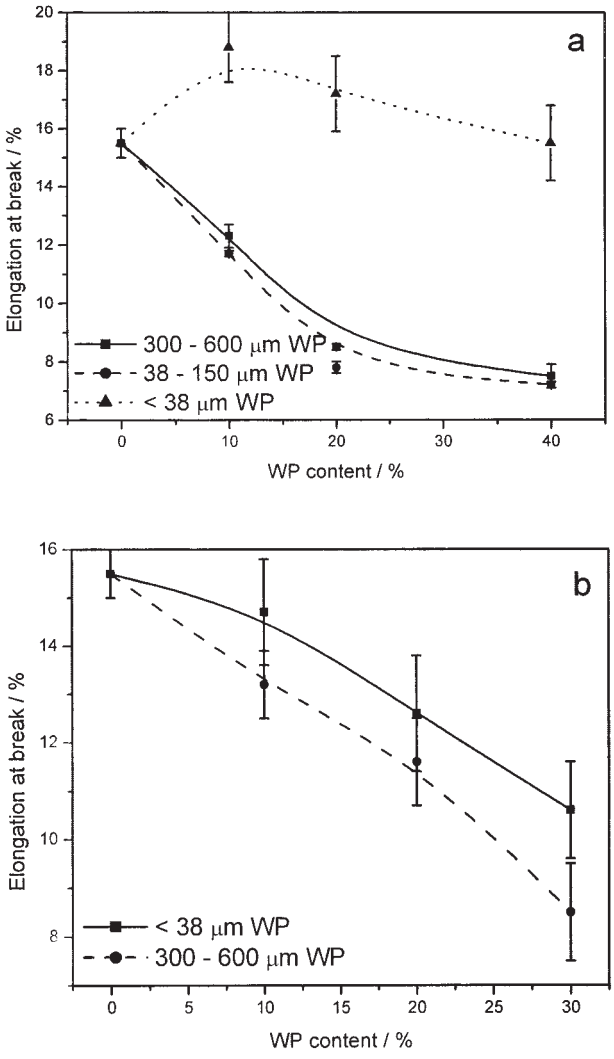

Figure 6 Elongation at break as function of WP content for (a) composites with different WP sizes and (b) composites with 10% MAPP.

TABLE V
Summarized Results for Tensile Properties

PP/MAPP/WP (w/w)	$\varepsilon_b \pm SE_b$ (%)	$\sigma_b \pm s\sigma_b$ (MPa)	$E \pm sE$ (MPa)
100/0/0	15.5 ± 0.5	30.4 ± 0.3	416.0 ± 16.7
90/0/10 (<38 μm)	18.8 ± 1.2	25.6 ± 0.4	418.8 ± 12.1
80/0/20 (<38 μm)	17.2 ± 1.3	22.7 ± 0.4	440.0 ± 10.9
60/0/40 (<38 μm)	15.5 ± 1.3	21.2 ± 0.3	445.1 ± 11.0
90/0/10 (38–150 μm)	11.7 ± 0.1	24.7 ± 0.4	492.0 ± 2.7
80/0/20 (38–150 μm)	7.8 ± 0.2	20.6 ± 0.5	510.0 ± 10.0
60/0/40 (38–150 μm)	7.2 ± 0.1	16.1 ± 0.4	500.0 ± 8.2
90/0/10 (300–600 μm)	12.3 ± 0.4	27.8 ± 0.2	451.9 ± 1.3
80/0/20 (300–600 μm)	8.5 ± 0.1	22.5 ± 0.4	510.4 ± 5.3
60/0/40 (300–600 μm)	7.5 ± 0.4	20.1 ± 0.7	498.2 ± 16.7
85/5/10 (<38 μm)	15.6 ± 2.6	26.2 ± 0.3	420.5 ± 22.6
80/10/10 (<38 μm)	14.7 ± 1.1	25.5 ± 1.1	362.3 ± 8.7
70/10/20 (<38 μm)	12.6 ± 0.0	26.1 ± 0.5	369.4 ± 9.0
60/10/30 (<38 μm)	10.6 ± 1.0	26.8 ± 0.4	410.0 ± 9.1
85/5/10 (38–150 μm)	14.5 ± 1.4	22.8 ± 0.7	494.1 ± 10.3
80/10/10 (38–150 μm)	14.3 ± 0.5	28.0 ± 0.7	494.9 ± 10.3
85/5/10 (300–600 μm)	15.8 ± 0.8	33.9 ± 1.1	499.0 ± 15.0
80/10/10 (300–600 μm)	13.2 ± 0.7	32.8 ± 0.7	512.0 ± 7.9
70/10/20 (300–600 μm)	11.6 ± 0.9	35.8 ± 0.6	573.1 ± 8.0
60/10/30 (300–600 μm)	8.5 ± 1.0	35.4 ± 0.8	570.2 ± 9.0

ε_b - elongation at break; σ_b - stress at break: E - Young's modulus.

adhesion is low and the material losses its toughness. It is known that the matrix adds toughness to a composite, and therefore an increase in filler content will result in a decrease in matrix content, resulting in a smaller amount of matrix to withstand the applied stress.[20] In the presence of MAPP the stress at break increases with increasing WP content for large WP particles, while it decreases for low contents of small WP particles, followed by a slight increase. This is probably the result of the location of MAPP at the interfaces between the phases and the enhancement of the stress transfer, resulting in an improvement of the mechanical properties.

Figure 8 shows an appreciable increase in Young's modulus with increasing WP content for composites with 38–150 μm and 300–600 μm WP particles. This is common behavior for polymer-filler composites, especially for composites filled with natural fillers. Fillers are said to be much stiffer than polymer matrices and as a result they add stiffness to the final product.[9] For the composites with 38 μm WP particles, there is only a slight increase in Young's modulus. In this case the small size allows more PP chain mobility. In the presence of MAPP the modulus shows the same trends than the stress at break.

CONCLUSIONS

From the discussion it is clear that WP size and content, as well as the presence of MAPP, play a significant role in the determination of the tensile properties, thermal stability and oxygen permeability of PP-WP composites. Generally the presence of MAPP gave rise

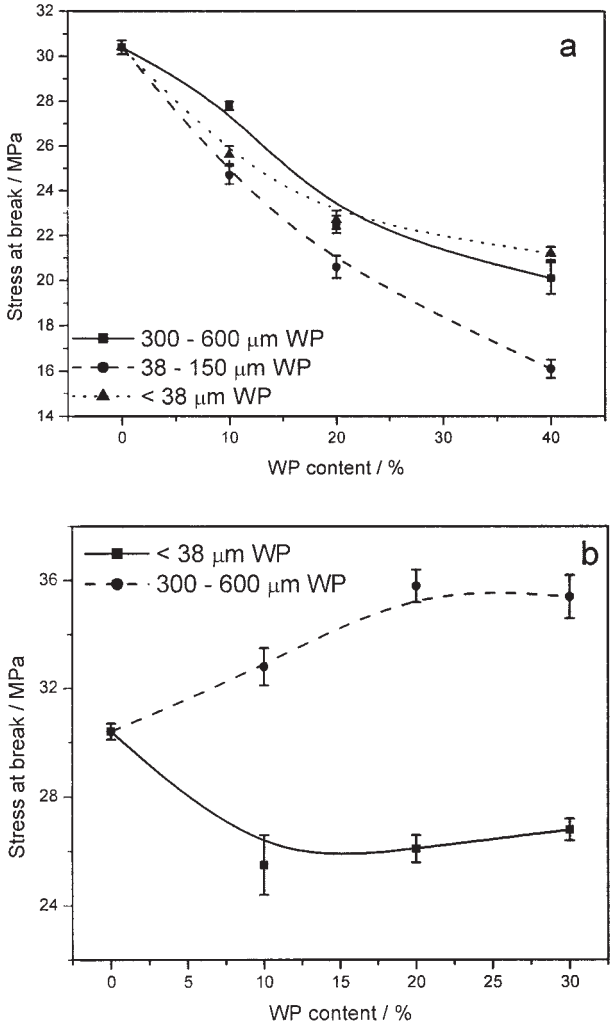

Figure 7 Stress at break as function of WP content for (a) composites with different WP sizes and (b) composites with 10% MAPP.

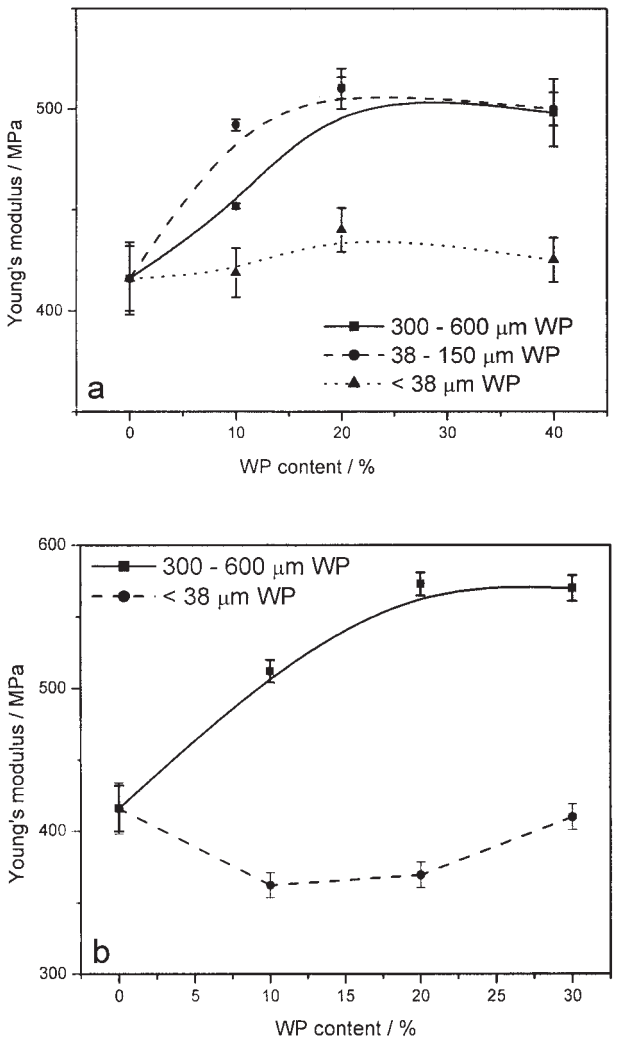

Figure 8 Young's modulus as function of WP content for (a) composites with different WP sizes and (b) composites with 10% MAPP.

to an improvement in all the investigated properties. This is to be expected because of the improved interaction between PP and WP in the presence of MAPP. It is, however, interesting to see that small WP particles give rise to improved properties, even in the absence of MAPP. For example, the PP composite containing 20 wt % WP (<38 μm) is thermally more stable than pure PP, has the lowest oxygen permeability of all investigated composites, has Young's modulus and elongation at break similar to those of pure PP, but has a higher stress at break than pure PP.

References

1. Thwe, M. M.; Liao, K. Compos A 2002, 33, 43.
2. Suarez, J. C. M.; Coutinho, F. M. B.; Sydenstricker, T. H. Polym Test 2003, 22, 819.
3. Kotch, J.; Kelnar, I.; Baldrian, J.; Raab, M. Eur Polym J 2004, 40, 679.
4. Hofmann, W. Rubber Technology Handbook; Hanser: Munich, 1989.
5. Fung, K. L.; Xing, Y. S.; Li, R. K. Y.; Tjong, S. C.; Mai, Y.-W. Compos Sci Technol 2003, 63, 1255.
6. Joseph, P. V.; Joseph, K.; Thomas, S.; Pillai, L. K. S.; Prasad, V. S.; Groeninckx, G.; Sarkisova, M. Compos A 2003, 34, 253.
7. Bueche, F. In Reinforcement of Elastomers; Kraus, G., Ed.; Interscience: New York, 1965.
8. Tang, B. In Proceedings of Fiber Reinforced Polymer Composites Applications; 1997.
9. Oksman, K.; Clemons, C. J Appl Polym Sci 1998, 67, 1503.
10. Pickering, K. L.; Abdalla, A.; Ji, C.; McDonald, A. G.; Franich, R. A. Compos A 2003, 34, 915.
11. Sain, M.; Park, S. H.; Suhara, F.; Law, S. Polym Degrad Stab 2004, 83, 363.
12. Wielage, B.; Lampke, Th.; Litschick, H.; Soergel, F. J Mater Process Technol 2003, 139, 140.
13. Sedlackova, M.; Lacik, I.; Chodak, I. Macromol Symp 2001, 170, 157.
14. Keneer, T. J.; Stuart, R. K.; Brown, T. K. Compos A 2004, 35, 357.
15. Herrera-Franco, P. J.; Valadez-Gonzalez, A. Compos A 2004, 35, 339.
16. Fu, S. Y.; Mai, Y.-W.; Ching, E. C. Y.; Li, R. K. Y. Compos A 2002, 33, 1549.
17. Simonse, J.; Jacobson, R.; Rowell, R. Forest Products J 1998, 48, 89.
18. Luo, S.; Netravali, A. N. J Mater Sci 1999, 34, 3709.
19. Wunderlich, B. Macromolecular Physics II; Academic Press: New York, 1973.
20. Oksman, K.; Lindberg, H. J Appl Polym Sci 1998, 68, 1845.